

See discussions, stats, and author profiles for this publication at: <https://www.researchgate.net/publication/230615279>

Unusually High-Performing Organic Field-Effect Transistors Based on π -Extended Semiconducting Porphyrins

ARTICLE in ADVANCED MATERIALS · OCTOBER 2012

Impact Factor: 17.49 · DOI: 10.1002/adma.201202148 · Source: PubMed

CITATIONS

24

READS

32

10 AUTHORS, INCLUDING:



Mai Ha Hoang

Institute of Chemistry, Vietnam Academy of...

29 PUBLICATIONS 310 CITATIONS

SEE PROFILE



Tae Wan Lee

Korea University

49 PUBLICATIONS 406 CITATIONS

SEE PROFILE



Suk Joong Lee

Korea University

61 PUBLICATIONS 2,282 CITATIONS

SEE PROFILE



Dong Hoon Choi

Korea University

283 PUBLICATIONS 2,498 CITATIONS

SEE PROFILE

Unusually High-Performing Organic Field-Effect Transistors Based on π -Extended Semiconducting Porphyrins

Mai Ha Hoang, Youngmee Kim, Minsik Kim, Kyung Hwan Kim, Tae Wan Lee, Duc Nghia Nguyen, Sung-Jin Kim, Kwangyeol Lee, Suk Joong Lee,* and Dong Hoon Choi*

Recently, the charge-transport phenomena of organic conjugated materials have been intensively investigated because of the potential applications of these materials in electronics and optoelectronics. Among these applications, organic field-effect transistors (OFETs) fabricated from either thin films or well-defined single crystals (SCs) as charge-transporting layers are the most promising electronic devices.^[1–5] In particular, the unique anisotropic arrangement of organic semiconducting molecules owing to their strong intermolecular interactions is expected to have a significant influence on the OFET performance, because the larger overlap of π -orbitals between neighboring molecules may increase the bandwidth and facilitate charge transport.^[6] In this regard, there has been considerable interest in the design and synthesis of planar π -conjugated molecules such as pentacene, oligothiophene, arylacetylene, indolo-[3,2-*b*]-carbazole, perylene, and tetrathiafulvalene for use in the fabrication of organic thin-film transistors (OTFTs).^[7] The molecular packing behaviors of these organic molecules are dominated by π - π interactions, leading to the formation of highly ordered polycrystalline films with good charge-transport properties.

Porphyrins are one of the most important π -conjugated planar molecules in the field of electronics and optoelectronics, and they have often been employed in OFETs,^[8] organic phototransistors (OPTs),^[9] and organic photovoltaics (OPVs).^[10] Because of their unique structure, porphyrins may provide multiple interactions such as hydrogen bonding, π - π stacking, electrostatic interactions, and metal-ligand coordination. However, the performances of recently developed porphyrin-based OFET

devices show relatively low carrier mobilities in the range of 10^{-6} to 10^{-1} cm² V⁻¹ s⁻¹.^[8] A deeper understanding of such systems has hardly been achieved because of the lack of information on the molecular packing and intermolecular arrangement (which are closely related to the OFET performance),^[11] since most porphyrin-based OFET devices are based on thin films or polycrystalline objects prepared by spin-coating or vacuum-deposition processes. Although porphyrin-based single-crystalline OFETs have been reported recently along with molecular arrangement studies, relatively poor device performances have been observed because of the restricted use of π -orbital conjugation.^[8a,e,f]

For a high degree of crystallinity with an excellent determinacy as well as a high corresponding device performance to be obtained, the extension of π -conjugation and the location of conjugative substituents on the porphyrin core may play major roles in terms of the molecular electronic energies and molecular arrangements during the formation of well-defined polycrystalline films or single crystals. Therefore, herein we report the new π -extended porphyrin derivatives H₂TP and ZnTP, consisting of a porphyrin core and four 2-ethynyl-5-hexylthiophene peripheral arms. We expected that such molecules would enable the best extension of π -conjugation and provide strong intermolecular π - π interactions.

H₂TP was readily obtained from a condensation reaction between 3-(5-hexylthiophen-2-yl)propionaldehyde and pyrrole in dichloromethane (DCM) with 14% yield. ZnTP was further obtained by metalation of H₂TP with Zn(OAc)₂ in quantitative yield (see the Supporting Information for detailed synthetic procedures (Scheme S1)). These materials were found to have good film-forming properties and high solubilities in various solvents such as chloroform, DCM, tetrahydrofuran (THF), and chlorobenzene at room temperature. In particular, density functional theory (DFT) calculations revealed that the planarity of the two-dimensionally conjugated unit was sustained, with a small degree of disorder around the hexyl substituents. Using simple slow diffusion of a solution of porphyrin in toluene over *n*-hexane, we were able to obtain microscopic crystalline objects. Optical microscopy analysis revealed these crystalline objects to be collections of fairly uniform needles with very high aspect ratios for both H₂TP and ZnTP; the widths ranged from several micrometers to tens of micrometers (Figure 1a,b).

The single-crystal X-ray crystallographic structures of H₂TP and ZnTP are shown in Figure 1c and 1d, respectively. As expected, the porphyrin cores in both H₂TP and ZnTP are nearly planar. Three thiophene rings are slightly tilted with respect to the N1/N2/N3/N4 porphyrin core plane (6.3(2)–10.7(2)° for H₂TP and 7.0(2)–12.2(2)° for ZnTP), and the

Dr. M. H. Hoang, Dr. M. Kim, Dr. K. H. Kim,
T. W. Lee, Prof. K. Lee, Prof. S. J. Lee,
Prof. D. H. Choi
Dept. of Chemistry,
Research Institute for Natural Sciences
Korea University
5 Anam-dong, Sungbuk-gu, Seoul 136-701, Korea
Fax: (+82)2-925-4284
E-mail: slee1@korea.ac.kr; dhchoi8803@korea.ac.kr
Dr. Y. Kim, Prof. S.-J. Kim
Department of Chemistry and NanoScience
Ewha Womans University
Seoul 136-701, Korea
Dr. M. H. Hoang, Prof. D. N. Nguyen
Institute of Chemistry
Vietnam Academy of Science and Technology
18 Hoang Quoc Viet, Cau Giay, Hanoi, Vietnam



DOI: 10.1002/adma.201202148

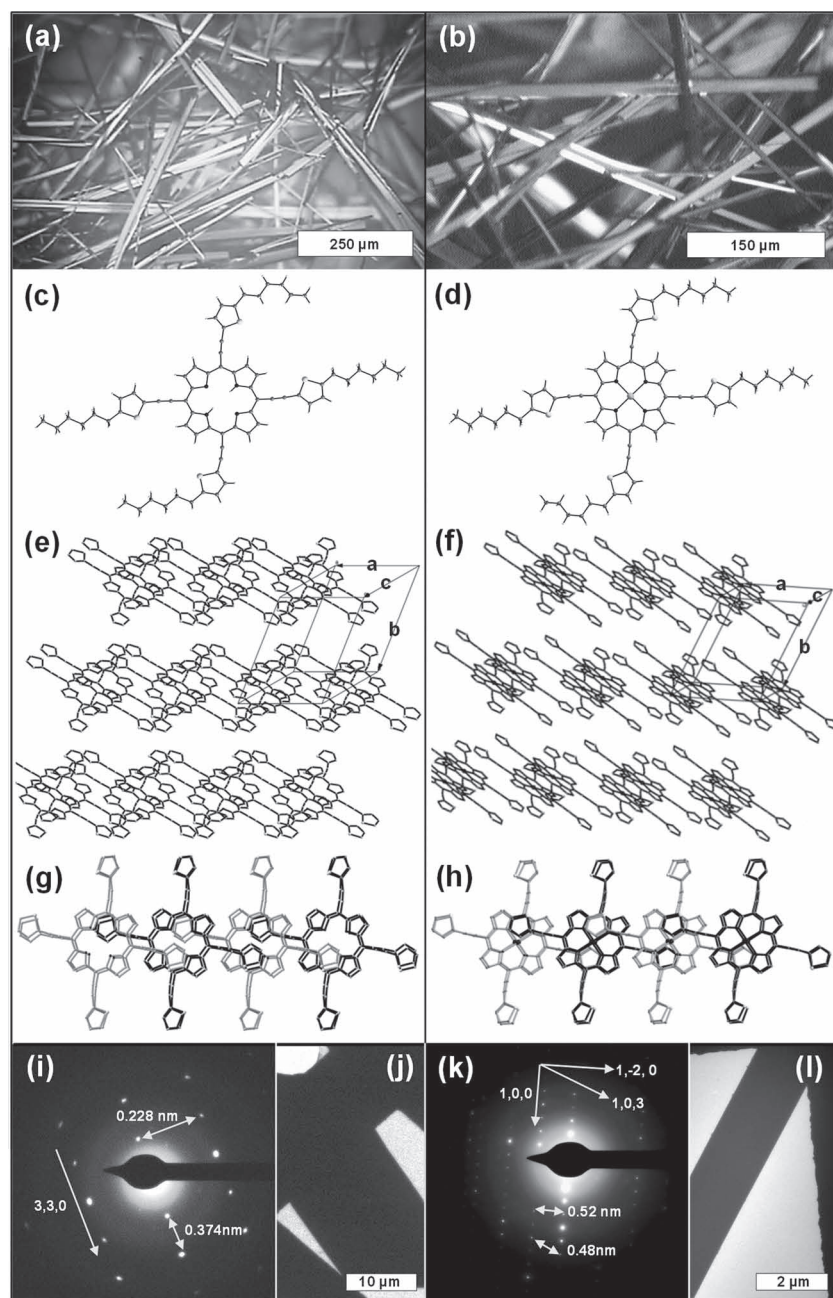


Figure 1. Optical microscopy images of needle crystals obtained from H₂TP (a) and ZnTP (b). Crystal structures (c and d), crystal packing diagrams (e and f), and co-facial packings (g and h) in the adjacent molecules (showing clear J-aggregation of H-aggregated molecular dimeric porphyrin pairs through π - π interaction) of H₂TP and ZnTP, respectively (hexyl groups in packing diagrams are omitted for clarity). SAED patterns and the corresponding TEM images of H₂TP (i and j) and ZnTP (k and l).

fourth tethered thiophene rings are tilted significantly from the porphyrin plane ($23.3(2)^\circ$ for H₂TP and $22.8(2)^\circ$ for ZnTP). Great similarities are found in the crystal structures (Table S2, Supporting Information) and crystal packing diagrams of these systems. In the packing diagram representations, two molecules act remarkably as a dimeric pair of porphyrins with a closest atom-atom distance of $3.29(5)$ Å for H₂TP (Figure 1e)

and an even shorter one ($3.06(3)$ Å) for ZnTP (Figure 1f). These porphyrin pairs are stacked in a dramatic staircase fashion through π - π interactions, with closest atom-atom distances of $3.37(3)$ Å for H₂TP and $3.34(3)$ Å for ZnTP. It should be pointed out that the H-aggregated dimeric pairs were aligned in a J-aggregation manner, which is capable of facilitating intermolecular carrier hopping and has slip-stacked carrier transport properties (Figure 1g, h). Furthermore, the distance between the porphyrins in these dimeric pairs is the shortest ever reported, and is comparable to that in a graphite layer ($d = 3.335$ Å).

Transmission electron microscopy (TEM) images and the corresponding selected-area electron diffraction (SAED) patterns of the H₂TP and ZnTP crystals were indexed based on triclinic cells, and the results agreed with the simulated powder patterns for the single crystals (Figure 1i, k). The SAED patterns were consistent throughout the whole crystal, indicating the single-crystalline nature of the needles.

The UV-vis absorption spectra of the solution, film, and crystal samples of H₂TP and ZnTP are shown in Figure 2. The solution samples were prepared in chloroform with a concentration of 1×10^{-6} M and the thin-film samples were fabricated by spin-coating the chloroform solutions of these molecules. The crystal samples were fabricated by spreading the crystals obtained from the slow diffusion of toluene solutions over *n*-hexane. A drastic spectral change was observed in the film and crystal states of these samples, which is attributed to the high degree of intermolecular interaction between the porphyrins. In particular, the absorption spectrum of the ZnTP crystal is significantly broadened and red-shifted, which is unequivocal evidence of the mixed formation of H-aggregated dimers and the J-aggregated set of molecules with the closest limited distances, supporting the above single-crystal results. The optical properties and energy levels are shown in Table S1, Supporting Information.

To examine their electrical characteristics, we investigated the charge-transport properties of H₂TP and ZnTP. OFETs (bottom-gate, top-contact) were fabricated on *n*-octyltrichlorosilane (OTS)-SiO₂/Si substrates, with N-doped polycrystalline silicon as the gate electrode, an OTS-treated SiO₂ surface layer as the dielectric gate insulator, and gold electrodes deposited using a shadow mask. The film devices were prepared by spin-coating chloroform solutions of the porphyrins, and the needle-crystal devices were prepared by the slow diffusion of toluene solutions over *n*-hexane. The devices were dried under vacuum

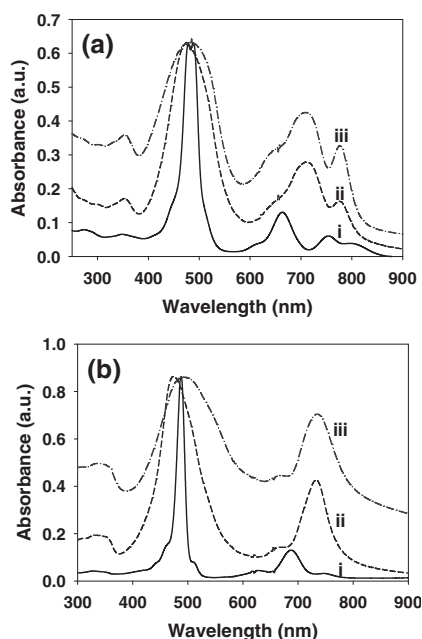


Figure 2. UV-Vis absorption spectra of solution (i), film (ii), and needle crystals (iii) of H₂TP (a) and ZnTP (b).

at room temperature for 24 h before testing at room temperature in air.

The insets in **Figure 3b** and **d** show the SEM images of each of the crystal FETs of H₂TP and ZnTP, where the channel lengths (widths) were 43.0 (1.5) and 89.0 (0.9) μm , respectively. The output characteristics showed very good saturation behaviors and clear saturation currents (see Figures S3–6, Supporting Information). The mobility values were obtained by measuring

more than 20 different devices. According to the transfer characteristics (**Figure 3**), the film devices made of H₂TP and ZnTP provided unusually high field-effect mobilities of 0.014 and 1.20 $\text{cm}^2 \text{V}^{-1} \text{s}^{-1}$, respectively, together with high on/off current ratios ($I_{\text{on/off}} = 5.0 \times 10^4$ and 1.5×10^8 , respectively) and low threshold voltages ($V_{\text{th}} \approx -5.0$ and -10.0 V, respectively). The crystalline-needle FETs made of H₂TP and ZnTP provided field-effect mobilities of 0.85 and 2.90 $\text{cm}^2 \text{V}^{-1} \text{s}^{-1}$, respectively, together with high on/off current ratios ($I_{\text{on/off}} = 1.0 \times 10^4$ and 6.0×10^3 , respectively) and threshold voltages ($V_{\text{th}} \approx 5.0$ and 2.0 V, respectively). To the best of our knowledge, these values are the highest yet reported for porphyrin-based OFET devices. The mobilities of these devices were well maintained (over 80–90% mobility compared with freshly prepared devices) even after three months' storage in air, showing that the devices have very good stabilities. Remarkably, the mobility of the H₂TP single-crystal device was 60 times higher than that of the film-state one, while the mobility of the ZnTP single-crystal device was 2.5 times higher than that of the film-state one. The dramatic increase in the mobility of the H₂TP single-crystal devices is presumably due to the denser molecular confinement, while the slight increase in mobility for the ZnTP single-crystal devices indicates that a highly and densely packed arrangement of polycrystallites has already been achieved in the solid film state (**Figure 3**).

Furthermore, FETs made of H₂TP and ZnTP displayed photoinduced enhancement of the source–drain current (I_{DS}). OPT devices of H₂TP (**Figure S7a**, Supporting Information) and ZnTP (**Figure 4a**) showed a dramatic increase in I_{DS} when illuminated with incident light. It should be emphasized that the drastic increase in I_{DS} was induced by the illumination of light in a broad range from 365 (UV) to 850 nm (near-IR) with a very low intensity (5.6 $\mu\text{W cm}^{-2}$). The large increase in drain current is ascribed to the trapped photogenerated electrons in the

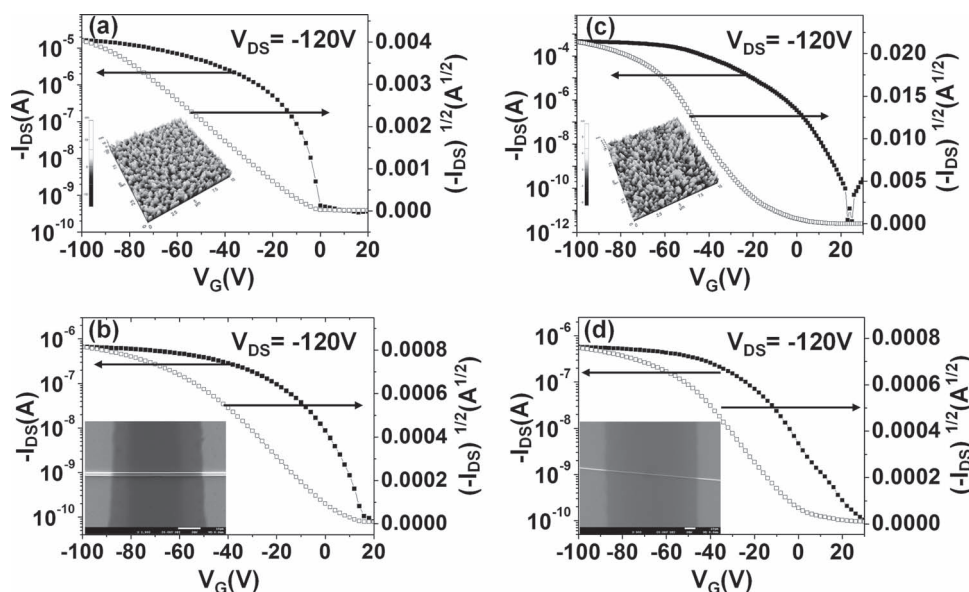


Figure 3. Electrical characterization of OFET devices. Transfer curves of thin film devices (a and c) and single crystal devices (b and d) made of H₂TP and ZnTP, respectively. (Inset: AFM images of TFT devices (a and c); SEM images of FET devices (b and d)).

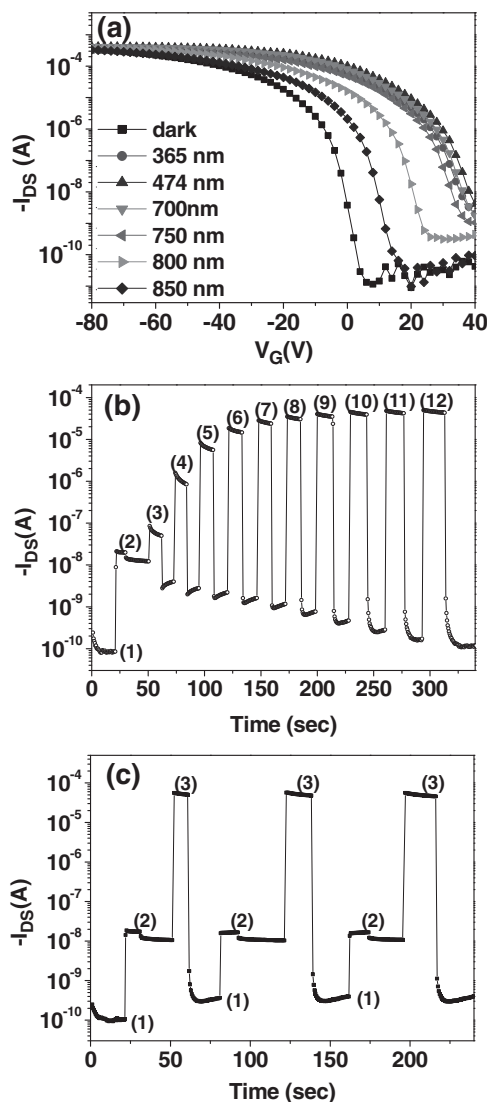


Figure 4. a) Transfer characteristics of ZnTP based-OPT in the dark and under monochromatic light irradiation ($I = 5.6 \mu\text{W cm}^{-2}$) with different wavelengths; b) Variation of I_{DS} with gate voltage (V_G); 1) light-on, 2) light-off, 3) $V_G = -10$ V, 4) $V_G = -20$ V, 5) $V_G = -30$ V, 6) $V_G = -40$ V, 7) $V_G = -50$ V, 8) $V_G = -60$ V, 9) $V_G = -70$ V, 10) $V_G = -80$ V, 11) $V_G = -90$ V, 12) $V_G = -100$ V; c) I_{DS} characteristics of photo-controlled optical memory operation, single-stage on-off memory under monochromatic light irradiation at $5.6 \mu\text{W cm}^{-2}$; 1) light-on (writing), 2) light-off (reading), and 3) $V_G = -100$ V (erasing).

semiconducting organic layer, which is close to the interface with the dielectric gate insulator. These trapped electrons have led to the injection and accumulation of additional holes in the active layer, thereby increasing the drain current.^[4d,e]

From the modulation of the transfer curve, we calculated the photoresponsivity (R) of the OPT device, defined as $\Delta I_{DS}/P_{inc}$, where ΔI_{DS} is $I_{DS,light} - I_{DS,dark}$ and P_{inc} is the incident light intensity. The photoswitching ratio (P) was obtained from $(I_{DS,light} - I_{DS,dark})/I_{DS,dark}$. The P and R values were determined near the crossing point of the two curves with $V_{DS} = -100$ V, $I = 5.6 \mu\text{W cm}^{-2}$, and $\lambda = 474$ nm, and are plotted in Figure S8, Supporting

Information. The OPT devices showed maximum P values of 4.4×10^4 ($V_G = -10.0$ V) for H_2TP and 4.6×10^6 ($V_G = -6.0$ V) for ZnTP, and exhibited a short response time on the application of both gate bias and incident light. The average R values of OPT devices were found to be $6.6 \times 10^2 \text{ AW}^{-1}$ ($V_G = -2.0$ V) for H_2TP and $2.2 \times 10^4 \text{ AW}^{-1}$ ($V_G = 2.0$ V) for ZnTP. The measured R values are significantly higher than those of inorganic single-crystal silicon FETs (300 AW^{-1} , $I = 30 \mu\text{W cm}^{-2}$).^[3a] It should be pointed out that the monochromatic light intensity employed in this study was very low compared to those reported in the literature (≈ 30 to 1 mW cm^{-2}).^[2-4] To the best of our knowledge, the R and P values obtained from this study are among the best yet found for OPT devices under such a low light intensity.

Once the photocurrent was generated, the I_{DS} levels could be steered by manipulating the gate voltage V_G during the light-off condition (Figure S7b for H_2TP and Figure 4b for ZnTP). When applying a negative V_G , an abrupt increase in I_{DS} was observed, indicating that photoinduced holes were accumulated at the interface between the insulator and the organic semiconductor. After the applied negative V_G was turned off, the photoinduced currents decreased rapidly to a certain level. As the absolute value of V_G increased, the resulting I_{DS} levels decreased because of the respective diminishing of the remnant photoinduced current. This observation motivated the application of these molecules in multi-stage photocontrolled memory.

Remarkably, OPTs made from these porphyrin molecules showed reproducible memory operations (Figure S7c for H_2TP and Figure 4c for ZnTP). The striking single-stage memory operation with gate bias is mainly due to the slow relaxation and trapping mechanism of the photoinduced charges. First, irradiation with low-intensity light ($I = 5.6 \mu\text{W cm}^{-2}$, $\lambda = 474$ nm) was used for the writing process (step (1)). The first on-state currents were measured ($I_{DS} = 2.4 \times 10^{-9}$ A for H_2TP and 1.06×10^{-8} A for ZnTP) in terms of the remnant photoinduced currents after the excitation light was turned off (step (2)). Secondly, erasing processes (step (3), $V_G = -100$ V) in the memory-effect curves were performed through a charge-trapping mechanism at the interface between the active and gate dielectric layers. Relatively high on/off current ratios were obtained (2.2×10^2 for H_2TP and 1.8×10^2 for ZnTP at $V_G = 0$ V) under initial light illumination.

In conclusion, we have demonstrated that the highly soluble new porphyrin derivatives H_2TP and ZnTP can be used to fabricate high-performance OFET and OPT devices from both thin films and single-crystalline needles, which can be obtained by scalable, low-cost solution processes. In particular, OFETs made from ZnTP displayed charge mobilities of up to $1.20 \text{ cm}^2 \text{ V}^{-1} \text{ s}^{-1}$ in the pristine films and $2.90 \text{ cm}^2 \text{ V}^{-1} \text{ s}^{-1}$ in single-crystal micro-objects with high on/off current ratios having the best values yet reported in the literature for metalloporphyrin-based materials. This high performance of the FETs is mainly due to the very intriguing J-aggregation of H-aggregated dimeric porphyrin pairs in the crystalline structures, resulting in stronger intermolecular π - π interactions incorporating unusually short layer distances, which enhance the charge-transport efficiency. Furthermore, the OPT devices of these molecules showed high photoresponsivities in a broad wavelength range from 365 (UV) to 850 nm (near-IR) under very low light intensity ($5.6 \mu\text{W cm}^{-2}$), making them potentially applicable for sensitive optoelectronic integrated devices. The results obtained in this work demonstrate

unambiguously the great potential of metalloporphyrins as candidates for future organic semiconducting materials.

Experimental Section

Crystal Data for H₂TP: C₆₈H₇₀N₄S₄, MW = 1071.52, Triclinic (P-1), $a = 12.583(3)$ Å, $b = 15.696(3)$ Å, $c = 16.681(3)$ Å, $\alpha = 71.26(3)^\circ$, $\beta = 85.87(3)^\circ$, $\gamma = 68.04(3)^\circ$, $V = 2889.2(10)$ Å³, $Z = 2$, (Mo K α) = 0.210 mm⁻¹, 16 119 reflections measured, 11 067 unique ($R_{\text{int}} = 0.0551$) which were used in all calculations, final $R = 0.0699$ ($R_w = 0.1523$) with reflections having intensities greater than 2σ , GOF (F^2) = 0.974. CCDC reference number: 868812.

Crystal Data for ZnTP: C₆₈H₆₈N₄S₄Zn, MW = 1134.87, Triclinic (P-1), $a = 12.528(3)$ Å, $b = 15.494(3)$ Å, $c = 16.701(3)$ Å, $\alpha = 72.16(3)^\circ$, $\beta = 86.59(3)^\circ$, $\gamma = 68.50(3)^\circ$, $V = 2866.1(10)$ Å³, $Z = 2$, (Mo K α) = 0.620 mm⁻¹, 16 138 reflections measured, 10 998 unique ($R_{\text{int}} = 0.0564$) which were used in all calculations, final $R = 0.0666$ ($R_w = 0.1363$) with reflections having intensities greater than 2σ , GOF (F^2) = 0.994. CCDC reference number: 868813.

Device Characterization: To characterize the FET performance, a bottom-gate top-contact device geometry was employed. H₂TP and ZnTP were dissolved in toluene and slow diffusion over *n*-hexane was employed to grow high quality crystalline needles on the surface of an OTS-treated SiO₂ insulator. The source and drain electrodes were then thermally evaporated (120 nm in thickness). All field effect mobilities were extracted in the saturation regime. The device performance was evaluated in air using a 4200-SCS semiconductor characterization system in ambient conditions. For the light source, a xenon lamp (Thermo Oriel) equipped with an optical fiber and high-speed monochromator (Oriel Cornerstone130 1/8 m Monochromator) were employed. The light illumination power was measured by using a Newport 2385-C Si photodetector with a calibration module.

Supporting Information

Supporting Information is available from the Wiley Online Library or from the author. CCDC 868812 for H₂TP and 868813 for ZnTP contain the supplementary crystallographic data for this paper. These data can be obtained free of charge from The Cambridge Crystallographic Data Centre via www.ccdc.cam.ac.uk/data_request/cif.

Acknowledgements

Support from the National Research Foundation of Korea (NRF20120002285 and 2012R1A2A1A01008797) and by Priority Research Centers Program through the National Research Foundation of Korea (NRF) funded by the Ministry of Education, Science and Technology (NRF20120005860).

Received: May 29, 2012

Published online: August 1, 2012

- [1] a) P. Gao, D. Beckmann, H. N. Tsao, X. Feng, V. Enkelmann, M. Baumgarten, W. Pisula, K. Müllen, *Adv. Mater.* **2009**, *21*, 213; b) L. Jiang, W. Hu, Z. Wei, W. Xu, H. Meng, *Adv. Mater.* **2009**, *21*, 3649; c) Y. Zhou, T. Lei, L. Wang, J. Pei, Y. Cao, J. Wang, *Adv. Mater.* **2010**, *22*, 1484.

- [2] a) S. R. Forrest, M. E. Thompson, *Chem. Rev.* **2007**, *107*, 923; b) Q. X. Tang, L. Q. Li, Y. B. Song, Y. L. Liu, H. X. Li, W. Xu, Y. Q. Liu, W. P. Hu, D. B. Zhu, *Adv. Mater.* **2007**, *19*, 2624; c) Y. Guo, C. Du, G. Yu, C.-A. Di, S. Jiang, H. Xi, J. Zheng, S. Yan, C. Yu, W. Hu, Y. Liu, *Adv. Funct. Mater.* **2010**, *20*, 1019.
- [3] a) N. M. Johnson, A. Chiang, *Appl. Phys. Lett.* **1984**, *45*, 1102; b) M. Y. Cho, S. J. Kim, Y. D. Han, D. H. Park, K. H. Kim, D. H. Choi, J. Joo, *Adv. Funct. Mater.* **2008**, *18*, 2905; c) Y.-Y. Noh, D.-Y. Kim, Y. Yoshida, K. Yase, B.-J. Jung, E. Lim, H.-K. Shim, *Appl. Phys. Lett.* **2005**, *86*, 043501; d) Y. Cao, Z. Wei, S. Liu, L. Gan, X. Guo, W. Xu, M. L. Steigerwald, Z. Liu, D. Zhu, *Angew. Chem. Int. Ed.* **2010**, *49*, 6319; e) X. Wang, K. Wasapinyokul, W. D. Tan, R. Rawcliffe, A. J. Campbell, D. D. C. Bradley, *J. Appl. Phys.* **2010**, *107*, 024509.
- [4] a) Y. Guo, C. Du, G. Yu, C.-a. Di, S. Jiang, H. Xi, J. Zheng, S. Yan, C. Yu, W. Hu, Y. Liu, *Adv. Funct. Mater.* **2010**, *20*, 1019; b) Q. Tang, L. Jiang, Y. Song, Y. Liu, H. Li, W. Xu, Y. Liu, W. Hu, D. Zhu, *Adv. Mater.* **2007**, *19*, 2624; c) J.-M. Choi, J. Lee, D. K. Hwang, J. H. Kim, S. Im, E. Kim, *Appl. Phys. Lett.* **2006**, *88*, 043508; d) K. H. Kim, S. Y. Bae, Y. S. Kim, J. A. Hur, M. H. Hoang, T. W. Lee, M. J. Cho, Y. Kim, M. Kim, J.-I. Jin, S.-J. Kim, K. Lee, S. J. Lee, D. H. Choi, *Adv. Mater.* **2011**, *23*, 3095; e) M. E. Gemayel, M. Treier, C. Musumeci, C. Li, K. Mullen, P. Samori, *J. Am. Chem. Soc.* **2012**, *134*, 2429.
- [5] a) V. C. Sundar, J. Zaumseil, V. Podzorov, E. Menard, R. L. Willett, T. Someya, M. E. Gershenson, J. A. Rogers, *Science* **2004**, *303*, 1644; b) J. Y. Lee, S. Roth, Y. W. Park, *Appl. Phys. Lett.* **2006**, *88*, 252106.
- [6] a) M. D. Curtis, J. Cao, J. W. Kampf, *J. Am. Chem. Soc.* **2004**, *126*, 4318; b) H. Moon, R. Zeis, E.-J. Borkent, C. Besnard, A. J. Lovinger, T. Siegrist, C. Kloc, Z. Bao, *J. Am. Chem. Soc.* **2004**, *126*, 15322.
- [7] a) M. M. Payne, S. R. Parkin, J. E. Anthony, C. C. Kuo, T. N. Jackson, *J. Am. Chem. Soc.* **2005**, *127*, 4986; b) A. Facchetti, Y. Deng, A. C. Wang, Y. Koide, H. Sirringhaus, T. J. Marks, R. H. Friend, *Angew. Chem. Int. Ed.* **2000**, *39*, 4547; c) V. A. L. Roy, Y. G. Zhi, Z. X. Xu, S. C. Yu, P. W. H. Chan, C. M. Che, *Adv. Mater.* **2005**, *17*, 1258; d) Y. L. Wu, Y. N. Li, S. Gardner, B. S. Ong, *J. Am. Chem. Soc.* **2005**, *127*, 614.
- [8] a) T. Minari, M. Seto, T. Nemoto, S. Isoda, K. Tsukagoshi, Y. Aoyagi, *Appl. Phys. Lett.* **2007**, *91*, 123501; b) C.-M. Che, H.-F. Xiang, S. S.-Y. Chui, Z.-X. Xu, V. A. L. Roy, J. J. Yan, W.-F. Fu, P. T. Lai, I. D. Williams, *Chem. Asian. J.* **2008**, *3*, 1092; c) Y.-Y. Noh, J.-J. Kim, K. Yase, S. Nagamatsu, *Appl. Phys. Lett.* **2003**, *83*, 1243; d) P. Ma, Y. Chen, N. Sheng, Y. Bian, J. Jiang, *Eur. J. Inorg. Chem.* **2009**, 954; e) P. Ma, Y. Chen, X. Cai, H. Wang, Y. Zhang, Y. Gao, J. Jiang, *Synth. Met.* **2010**, *160*, 510; f) M. H. Hoang, Y. Kim, S.-J. Kim, D. H. Choi, S. J. Lee, *Chem. Eur. J.* **2011**, *17*, 7772.
- [9] a) H.-X. Ji, J.-S. Hu, L.-J. Wan, *Chem. Commun.* **2008**, 2653; b) M. H. Sayyad, Z. Ahmad, K. S. Karimov, M. Yaseen, M. Ali, *J. Phys. D: Appl. Phys.* **2009**, *42*, 105112.
- [10] a) H. Imahori, S. Fukuzumi, *Adv. Funct. Mater.* **2004**, *14*, 525; b) Y. Shao, Y. Yang, *Adv. Mater.* **2005**, *17*, 2841; c) Z.-X. Xu, V. A. L. Roy, Z.-T. Liu, C. S. Lee, *Appl. Phys. Lett.* **2010**, *97*, 163301; d) M. D. Perez, C. Borek, P. I. Djurovich, E. I. Mayo, R. R. Lunt, S. R. Forrest, M. E. Thompson, *Adv. Mater.* **2009**, *21*, 1517; e) Y. Li, Y. Bian, M. yan, P. S. Thapaliya, D. Johns, X. Yan, D. Galipeau, J. Jiang, *J. Mater. Chem.* **2011**, *21*, 11131.
- [11] a) H. Sirringhaus, *Adv. Mater.* **2005**, *17*, 2411; b) Z. Wei, W. Hong, H. Geng, C. Wang, Y. Liu, R. Li, W. Xu, Z. Shuai, W. Hu, Q. Wang, D. Zhu, *Adv. Mater.* **2010**, *22*, 2458; c) L. Jiang, W. Hu, Z. Wei, W. Xu, H. Meng, *Adv. Mater.* **2009**, *21*, 3649; d) H. E. Katz, Z. Bao, S. L. Gilat, *Acc. Chem. Res.* **2001**, *34*, 359.